

Online Zeroth-order Optimisation on Riemannian Manifolds

Alejandro I. Maass, Chris Manzie, Dragan Nešić, Jonathan H. Manton, Iman Shames

Department of Electrical and Electronic Engineering
The University of Melbourne, Australia

e-mails: {alejandro.maass,manziec,dnesic,jmanton,iman.shames}@unimelb.edu.au

Abstract

We study numerical optimisation algorithms that use zeroth-order information to minimise time-varying geodesically-convex cost functions on Riemannian manifolds. In the Euclidean setting, zeroth-order algorithms have received a lot of attention in both the time-varying and time-invariant case. However, the extension to Riemannian manifolds is much less developed. We focus on Hadamard manifolds, which are a special class of Riemannian manifolds with global nonpositive curvature that offer convenient grounds for the generalisation of convexity notions. Specifically, we derive bounds on the expected instantaneous tracking error, and we provide algorithm parameter values that minimise a metric of performance. Our results illustrate how the manifold geometry in terms of the sectional curvature affects these bounds. To the best of our knowledge, these are the first error bounds for online zeroth-order Riemannian optimisation. Lastly, via numerical simulations, we demonstrate the applicability of our algorithm on an online Karcher mean problem.

1 Introduction

Time-varying optimisation problems are popular in the machine learning community under the framework known as *online convex optimisation* (OCO) (Hazan, 2019). OCO is a promising methodology for modelling sequential tasks, and the main goal is developing algorithms that can track trajectories of the optimisers of the time-varying optimisation problem (up to asymptotic error bounds). We refer the reader to (Simonetto et al., 2020) for a review of available algorithms and applications. In this paper, we study the following sequence of optimisation problems

$$\min_{x \in \mathcal{X}_{\mathcal{C}\mathcal{M}}} f_k(x), \quad (1)$$

where \mathcal{M} is a Hadamard submanifold embedded in \mathbb{R}^n , \mathcal{X} is a closed geodesically convex set, and f_k belongs to the class of continuous functions $\mathcal{F} := \{f_k : \mathcal{M} \rightarrow \mathbb{R} \mid k \in \mathbb{K}\}$, where¹

$$\mathbb{K} := \mathbb{N}_0 \cup \left\{j + \frac{1}{2} \mid j \in \mathbb{N}_0\right\} = \{0, 1/2, 1, 3/2, 2, 5/2, \dots\},$$

and every $\{f_k\}_{k \in \mathbb{K}} \in \mathcal{F}$ is geodesically L -smooth and geodesically strongly convex (see Definitions 2 and 3 further below). Hadamard manifolds are a special class of Riemannian manifolds that provide proper grounds for the generalisation of convexity notions from the Euclidean setting to nonlinear spaces (Bacák, 2014). Technically speaking, Hadamard manifolds are Riemannian manifolds that

¹The same class of functions was considered in (Shames et al., 2019) for the Euclidean setting $\mathcal{M} \equiv \mathbb{R}^n$.

are complete, simply connected, and with global nonpositive curvature (Bishop and O’Neill, 1969)—we define these concepts formally in Section 2. Some classical examples include hyperbolic spaces, manifolds of positive definite matrices, and \mathbb{R}^n .

We assume that the analytical form of the functions $\{f_k\}_{k \in \mathbb{K}}$ and their gradients are not available, and we can only obtain function evaluations via a zeroth-order oracle. Each cost function is thus seen as a black-box with time-varying input-output map. This scenario is found in many applications where derivatives are either unavailable, or too expensive to compute, see e.g. machine learning (Malik et al., 2019; Mania et al., 2018), online controller tuning (Ira et al., 2020), deep neural networks (Chen et al., 2017), and mobile fog computing (Chen and Giannakis, 2018).

Consequently, we aim to generate solutions to (1) using random gradient-free iterates of the form

$$x_{k+1} = \mathcal{P}_{\mathcal{X}} \left[\text{Exp}_{x_k}(-\alpha_k g_{\eta, k^+}(x_k, u_k)) \right], \quad (2)$$

where $\mathcal{P}_{\mathcal{X}}$ denotes the projection that maps a point $x \in \mathcal{M}$ to $\mathcal{P}_{\mathcal{X}}(x) \in \mathcal{X} \subset \mathcal{M}$ such that $\text{dist}(x, \mathcal{P}_{\mathcal{X}}(x)) < \text{dist}(x, y)$, for all $y \in \mathcal{X} \setminus \{\mathcal{P}_{\mathcal{X}}(x)\}$, and $\mathcal{P}_{\mathcal{X}}(x) = x$ for $x \in \mathcal{X}$. The positive constant α_k denotes the step size, g_{η, k^+} is the oracle, and $\text{Exp}_{x_k}(\cdot)$ denotes the exponential mapping which we define further below. We consider an extension of the recently proposed zeroth-order oracle for optimisation over Riemannian manifolds in (Li et al., 2020) to make it suitable for our online optimisation setting. That is,

$$g_{\eta, k^+}(x, u) := \frac{f_{k^+}(\text{Exp}_x(\eta u)) - f_k(x)}{\eta} u, \quad (3)$$

where $k^+ := k + 1/2$, $u = Pu_0 \in T_x \mathcal{M}$, $u_0 \sim \mathcal{N}(0, I_n) \in \mathbb{R}^n$, and $P \in \mathbb{R}^{n \times n}$ is the orthogonal projection matrix onto the tangent space $T_x \mathcal{M}$ of \mathcal{M} at x . We note that the proposed oracle is based on the one recently introduced in (Li et al., 2020) for time-invariant cost functions; however, ours allows for f to be time-varying as per our class of functions \mathcal{F} . Note that we are using a particular case of the general retraction $R_x(\eta u)$ in (Li et al., 2020) which is the exponential mapping $\text{Exp}_x(\eta u)$.

1.1 Related work

Our work lies in the general field of optimisation over Riemannian manifolds which has received a lot of attention recently in the literature given its applications to machine learning (Zhang et al., 2016), signal processing (Manton, 2002), dictionary learning (Sun et al., 2016), and low-rank matrix completion (Vandereycken, 2013), among others. For the time-invariant—or *offline*—setting, several results have been proposed in the literature, and we briefly review them below. For instance, Boumal et al. (2019) provided convergence rates for deterministic Riemannian gradient descent and smooth cost functions. Stochastic algorithms were also considered for smooth Riemannian optimisation in (Bonnabel, 2013; Kasai et al., 2018; Weber and Sra, 2019; Zhang et al., 2016; Zhou et al., 2019). Particularly, Bonnabel (2013) extended the classical stochastic gradient descent algorithms to the Riemannian case, and provided convergence results. Zhang et al. (2016) introduced the variance-reduced RSVRG method and considered Riemannian optimisation of finite sums of geodesically smooth functions. Kasai et al. (2018) proposed a Riemannian stochastic recursive gradient algorithm (RSRG) which provides notable computational advantages in comparison to RSVRG. Zhou et al. (2019) introduced the Riemannian SPIDER method for non-convex Riemannian optimisation as a simple and efficient extension of the Euclidean SPIDER counterpart. Lastly, Weber and Sra (2019) studied stochastic projection-free methods for constrained optimisation of smooth functions on Riemannian manifolds. The stochastic Riemannian Frank-Wolfe methods for

nonconvex and geodesically convex problems are introduced. For non-smooth cost functions, Riemannian subgradient methods have been proposed in (Li et al., 2019), manifold ADMM methods in (Kovnatsky et al., 2016), manifold proximal gradient (MANPG) methods in (Chen et al., 2020), manifold proximal point algorithms (MANPPA) in (Chen et al., 2019), and stochastic MANPG in (Wang et al., 2020).

None of the aforementioned works have considered the zeroth-order setting, in which the oracle makes available only cost function values as opposed to first-order or second-order information. To the best of our knowledge, zeroth-order Riemannian optimisation for time-invariant cost functions have been considered in (Chattopadhyay et al., 2015; Fong and Tino, 2019; Li et al., 2020). Particularly, Fong and Tino (2019) presented the extended Riemannian stochastic derivative-free optimisation (RSDFO) algorithm, and proved it converges in finitely many steps in compact connected Riemannian manifolds. Chattopadhyay et al. (2015) extended the Powell’s derivative-free optimisation method in (Powell, 1964) to Riemannian manifolds, but did not provide any complexity or convergence results. Just recently, the paper (Li et al., 2020) provided the first complexity results for both deterministic and stochastic zeroth-order Riemannian optimisation. Their zeroth-order methods rely on an estimator of the Riemannian gradient based on a modification of the Gaussian smoothing technique from the seminal work by Nesterov and Spokoiny (2017).

We note that the existing works on zeroth-order Riemannian optimisation listed above do not consider the online setting (1) in which the cost-function is allowed to be time-varying. This problem, however, has been widely studied for $\mathcal{M} \equiv \mathbb{R}^n$, see e.g. (Besbes et al., 2015; Bubeck and Cesa-Bianchi, 2012; Chiang et al., 2013; Dixit et al., 2019; Yang et al., 2016), in which it is assumed that cost function evaluations are carried out simultaneously when computing two-point estimates of the gradient. Later in (Shames et al., 2019), this assumption was relaxed and the cost function was allowed to change between function evaluations, which added an extra modelling layer that better respects the time-varying nature of the problem.

1.2 Contributions

Our contributions are threefold:

- We extend the OCO framework presented in (Shames et al., 2019) from the Euclidean setting to the case where the cost function is defined on a Hadamard manifold. Our proposed algorithm uses an extension of the zeroth-order oracle recently presented by Li et al. (2020) that allows for the function to be time-varying.
- We provide asymptotic bounds on the expected instantaneous tracking error, which to the best of our knowledge, are the first error bounds for online zeroth-order optimisation on Riemannian manifolds available in the literature. Our results illustrate how the manifold geometry—in terms of the sectional curvature—influences the performance of the algorithm.
- We provide choices for the algorithm parameters—step size and oracle’s precision—such that the asymptotic error bound is minimised, which is the chosen measure of performance. In addition, we give some remarks on regret bounds which open the door to interesting future directions.

2 Preliminaries

In this section, we present a brief introduction on the basics of manifold optimization. For a more in-depth revision we refer the reader to (Absil et al., 2009). A smooth manifold is a topological

manifold \mathcal{M} with a globally defined differentiable structure. At any point x on a smooth manifold, tangent vectors are defined as the tangents of parametrised curves passing through x . The tangent space $T_x\mathcal{M}$ of a manifold \mathcal{M} at x is defined as the set of all tangent vectors at the point x . Tangent vectors on manifolds generalise the notion of a directional derivative. Formally, we can define the tangent space $T_x\mathcal{M}$ as follows

$$T_x\mathcal{M} := \{\gamma'(0) : \gamma(0) = x, \gamma([- \varepsilon, \varepsilon]) \subset \mathcal{M} \text{ for some } \varepsilon > 0, \gamma \text{ is differentiable}\}.$$

The tangent bundle of a differentiable manifold \mathcal{M} is the manifold $T\mathcal{M}$ that assembles all the tangent vectors in \mathcal{M} . As a set, it is the disjoint union of all the tangent planes, i.e. $T\mathcal{M} := \sqcup_{x \in \mathcal{M}} T_x\mathcal{M}$. The dimension of a manifold \mathcal{M} , denoted as d , is the dimension of the Euclidean space that the manifold is locally homeomorphic to. In particular, the dimension of the tangent space is always equal to the dimension of the manifold.

A Riemannian manifold is a couple (\mathcal{M}, g) , where \mathcal{M} is a smooth manifold equipped with a smoothly varying inner product (Riemannian metric) on the tangent space at every point, i.e. $g(\cdot, \cdot) := \langle \cdot, \cdot \rangle_x : T_x\mathcal{M} \times T_x\mathcal{M} \rightarrow \mathbb{R}$. Without loss of generality, when the Riemannian metric is clear from the context, we simply talk about “the Riemannian manifold \mathcal{M} ”. Throughout, we assume the Levi-Civita connection is associated with (\mathcal{M}, g) .

Definition 1 (Riemannian gradient) *Suppose f is a smooth function on the Riemannian manifold \mathcal{M} . The Riemannian gradient $\text{grad}f(x)$ is defined as the unique element of $T_x\mathcal{M}$ satisfying $\langle \xi, \text{grad}f(x) \rangle_x = \frac{d}{dt}f(\gamma(t))|_{t=0}$ for any $\xi \in T_x\mathcal{M}$, where $\gamma(t)$ is a curve in \mathcal{M} such that $\gamma(0) = x$ and $\gamma'(0) = \xi$.*

A Riemannian submanifold \mathcal{M} of a Riemannian manifold \mathcal{N} is a submanifold of \mathcal{N} equipped with the Riemannian metric inherited from \mathcal{N} . Since in this paper we assume that \mathcal{M} is a Riemannian submanifold embedded in \mathbb{R}^n , \mathcal{M} is equipped with the Riemannian metric inherited from \mathbb{R}^n . We thus write the inner product on the tangent space $\langle \cdot, \cdot \rangle_x$ at every point $x \in \mathcal{M}$ as $\langle \cdot, \cdot \rangle_x = \langle \cdot, \cdot \rangle$, with the right-hand side being the Euclidean inner-product. Consequently, the Riemannian gradient in Definition 1 becomes the projection of its Euclidean gradient onto the tangent space, that is $\text{grad}f(x) = \mathcal{P}_{T_x\mathcal{M}}(\nabla f(x))$, where $\nabla f(x)$ denotes the Euclidean gradient of f at x .

We now introduce a family of local parametrisations often called *retractions*. In a nutshell, retractions allow us to move on a manifold (i.e. move in the direction of a tangent vector) while staying on the manifold. Formally, we say that a retraction mapping R_x is a smooth mapping from $T_x\mathcal{M}$ to \mathcal{M} such that $R_x(0) = x$, and the differential at 0 is an identity mapping, i.e. $\frac{d}{dt}R_x(t\xi)|_{t=0} = \xi$, for all $\xi \in T_x\mathcal{M}$. We refer to the latter as the local rigidity condition. In other words, for every tangent vector $\xi \in T_x\mathcal{M}$, the curve $\gamma_\xi : t \mapsto R_x(t\xi)$ satisfies $\dot{\gamma}_\xi(0) = \xi$. Moving along the curve γ_ξ is thought of as moving in the direction ξ while constrained to the manifold \mathcal{M} . In particular, the exponential mapping Exp_x is a retraction that generates geodesics. A geodesic is a curve representing in some sense the shortest path between two points in a Riemannian manifold.

Throughout this paper, we assume that \mathcal{M} is a Hadamard manifold, which is a special type of Riemannian manifold. A Hadamard manifold is complete, simply connected, and has nonpositive sectional curvature everywhere (Bacák, 2014; Bishop and O’Neill, 1969). Complete refers to the domain of the exponential mapping being the whole tangent bundle $T\mathcal{M}$, and simply connected means there are no circular paths that cannot be shrunk to a point. Hadamard manifolds have strong properties. For instance, there exists a unique geodesic between any two points on \mathcal{M} , and the exponential map is globally invertible at any point, $\text{Exp}_x^{-1} : \mathcal{M} \rightarrow T_x\mathcal{M}$. The geodesic distance is thus given by $\text{dist}(x, y) = \|\text{Exp}_x^{-1}(y)\| = \|\text{Exp}_y^{-1}(x)\|$, where $\|\cdot\|$ is the norm associated with the Riemannian metric, which in our setting corresponds to the Euclidean norm as discussed above. On

a Hadamard manifold, the notion of parallel transport provides a way to transport a vector along a geodesic. It is defined as the operator $\Gamma_x^y : T_x\mathcal{M} \rightarrow T_y\mathcal{M}$ which maps $v \in T_x\mathcal{M}$ to $\Gamma_x^y(v) \in T_y\mathcal{M}$ while preserving the inner product, i.e. $\langle u, v \rangle_x = \langle \Gamma_x^y(u), \Gamma_x^y(v) \rangle_y$.

We introduce some important definitions for our class of cost functions.

Definition 2 (Geodesically L -smoothness) *A differentiable function $f \in \mathcal{F}$ is said to be geodesically L -smooth if there exists $L \geq 0$ such that the following inequality holds for all $x, y \in \mathcal{M}$,*

$$\|\text{grad}f(x) - \Gamma_y^x(\text{grad}f(y))\| \leq L\text{dist}(x, y), \quad (4)$$

where we recall that $\text{dist}(x, y)$ denotes the geodesic distance between x and y , and Γ_y^x is the parallel transport from y to x .

It can be shown that if f is geodesically L -smooth, then for any $x, y \in \mathcal{M}$ we have (Zhang and Sra, 2016; Zhou et al., 2019)

$$f(y) \leq f(x) + \langle \text{grad}f(x), \text{Exp}_x^{-1}(y) \rangle_x + \frac{L}{2}\text{dist}(x, y)^2. \quad (5)$$

Definition 3 (Geodesic strong convexity) *A function $f \in \mathcal{F}$ is said to be geodesically σ -strongly convex if there exists $\sigma \in (0, L]$ such that for any $x, y \in \mathcal{M}$,*

$$f(y) \geq f(x) + \langle \text{grad}f(x), \text{Exp}_x^{-1}(y) \rangle_x + \frac{\sigma}{2}\text{dist}(x, y)^2.$$

Throughout this paper, the expectation operator is defined as $\mathbb{E}[g(u_0)] := \frac{1}{\nu} \int_{\mathbb{R}^n} g(u_0) e^{-\frac{1}{2}\|u_0\|^2} du_0$, where ν is the normalising constant, see also (Li et al., 2020).

3 Online optimisation using zeroth-order Riemannian oracles

Before presenting our results we state the underlying assumptions.

Assumption 1

- (a) Every $f \in \mathcal{F}$ in (1) is geodesically L -smooth and geodesically strongly convex as per Definitions 2 and 3, respectively.
- (b) $\exists V \geq 0$ such that $\text{dist}(x_{k+1}^*, x_{k+}^*) \leq V$, where $x_k^* := \arg \min_{x \in \mathcal{M}} f_k(x)$ for all $k \in \mathbb{K}$.
- (c) $\exists \delta > 0$ such that $|f_k(x) - f_{k+}(x)| \leq \delta$ for all $x \in \mathcal{M}$.
- (d) The sectional curvature of \mathcal{M} is lower-bounded by $\kappa \leq 0$.
- (e) $\exists R > 0$ such that $\max_{y, z \in \mathcal{X}} \text{dist}(y, z) \leq R$.

Similar assumptions have been used in the literature when $\mathcal{M} \equiv \mathbb{R}^n$, see e.g. (Dixit et al., 2019; Shames et al., 2019). Particularly, (a) generalises assumptions such as Lipschitz gradient smoothness and strong convexity often adopted in convex optimisation over \mathbb{R}^n . Item (b) bounds the change in minimiser, and (c) bounds the variation between consecutive cost functions. Note that $\delta \rightarrow 0$ corresponds to the special case where the cost-function does not vary between evaluations and thus $g_{\eta, k+}(x, u) = g_{\eta, k}(x, u)$ in (3). Lastly, (d) assumes a lower bound in the curvature of

\mathcal{M} , and (e) an upper bound in the diameter of \mathcal{X} , which are common assumptions in Riemannian optimisation see e.g. (Bonnabel, 2013; Li et al., 2020; Zhang and Sra, 2016).

We note that since $f \in \mathcal{F}$ is geodesically strongly convex as per Assumption 1(a), it is immediate to show that each $f \in \mathcal{F}$ satisfies

$$-\langle \text{grad}f(x), \text{Exp}_x^{-1}(x^*) \rangle \geq \frac{\sigma}{2} \text{dist}(x, x^*)^2, \quad (6)$$

for all $x \in \mathcal{M}$, where $x^* := \arg \min_{x \in \mathcal{M}} f(x)$. We will use this inequality in our analysis further below. Inequality (6) is the Riemannian counterpart of the restricted secant inequality in \mathbb{R}^n .

3.1 Error bounds

We define the *tracking error* as

$$e_k := \text{dist}(x_k, x_{k+}^*) = \|\text{Exp}_{x_k}^{-1}(x_{k+}^*)\| = \|\text{Exp}_{x_{k+}^*}^{-1}(x_k)\|,$$

and the *estimation error* as

$$\bar{e}_k := \text{dist}(x_{k+1}, x_{k+}^*) = \|\text{Exp}_{x_{k+1}}^{-1}(x_{k+}^*)\| = \|\text{Exp}_{x_{k+}^*}^{-1}(x_{k+1})\|.$$

The objects e_k and \bar{e}_k are also known as *pre-update optimality gap* and *post-update optimality gap*, respectively, see e.g. (Dixit et al., 2019). A common technique for analysing optimisation algorithms is to write the estimation error in terms of the tracking error by using the law of cosines in the Euclidean space. However, this equality does not exist for general nonlinear spaces, and in fact, there are no corresponding analytical expressions. However, Zhang and Sra (2016) have proposed a trigonometric distance bound for Alexandrov spaces with curvature bounded below. Alexandrov spaces are length spaces with curvature bound and form a generalisation of Riemannian manifolds with sectional curvature bounded below. The result uses the properties of *geodesic triangles*, and it can be used as an analogue to the law of cosines given its fundamental nature.

Lemma 1 *For any Riemannian manifold \mathcal{M} with a sectional curvature lower bounded by κ , and any points $x_{k+}^*, x_k \in \mathcal{M}$, the update $x_{k+1} = \mathcal{P}_{\mathcal{X}}[\text{Exp}_{x_k}(-\alpha_k g_{\eta, k+}(x_k, u_k))]$ satisfies*

$$\bar{e}_k^2 \leq e_k^2 + 2\alpha_k \langle g_{\eta, k+}(x_k, u_k), \text{Exp}_{x_k}^{-1}(x_{k+}^*) \rangle + \zeta(\kappa, e_k) \alpha_k^2 \|g_{\eta, k+}(x_k, u_k)\|^2, \quad (7)$$

where $\zeta(\kappa, e_k) := e_k \sqrt{|\kappa|} / \tanh(e_k \sqrt{|\kappa|})$.

Proof Let $\tilde{x}_{k+1} := \text{Exp}_{x_k}(-\alpha_k g_{\eta, k+}(x_k, u_k))$, and consider the geodesic triangle depicted in Figure 1 with vertices x_{k+}^*, x_k , and \tilde{x}_{k+1} , and sides $a := \text{dist}(\tilde{x}_{k+1}, x_{k+}^*)$, $b := \text{dist}(x_k, \tilde{x}_{k+1})$, and $c := e_k = \text{dist}(x_k, x_{k+}^*) = \|\text{Exp}_{x_k}^{-1}(x_{k+}^*)\|$. For this triangle, we have that $\text{dist}(x_k, \tilde{x}_{k+1}) = \|\text{Exp}_{x_k}^{-1}(\tilde{x}_{k+1})\| = \alpha_k \|g_{\eta, k+}(x_k, u_k)\|$. In addition, we have that

$$bc \cos(A) = \langle -\alpha_k g_{\eta, k+}(x_k, u_k), \text{Exp}_{x_k}^{-1}(x_{k+}^*) \rangle.$$

Then, by Lemma 5,

$$\text{dist}(\tilde{x}_{k+1}, x_{k+}^*)^2 \leq e_k^2 + 2\alpha_k \langle g_{\eta, k+}(x_k, u_k), \text{Exp}_{x_k}^{-1}(x_{k+}^*) \rangle + \zeta(\kappa, e_k) \alpha_k^2 \|g_{\eta, k+}(x_k, u_k)\|^2. \quad (8)$$

Lastly, note that by Lemma 2, $\text{dist}(\tilde{x}_{k+1}, x_{k+}^*)^2 \geq \text{dist}(x_{k+1}, x_{k+}^*)^2 = \bar{e}_k^2$, and thus the result follows immediately from (8). \blacksquare

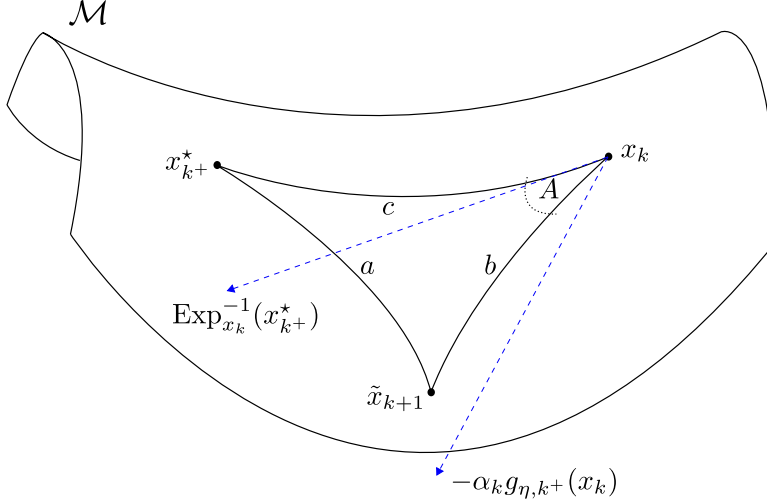


Figure 1: Illustration of the geodesic triangle used in Lemma 5.

We also derive a relation between the conditional expectations of e_{k+1} and \bar{e}_k . By Assumption 1(b) and the triangle inequality for the geodesic distance $\text{dist}(\cdot, \cdot)$, we can write

$$\begin{aligned}
 e_{k+1} &= \text{dist}(x_{k+1}, x_{k+1}^*) \\
 &\leq \text{dist}(x_{k+1}, x_{k+}^*) + \text{dist}(x_{k+}^*, x_{k+1}^*) \\
 &\leq \bar{e}_k + 2V \\
 \mathbb{E}[e_{k+1} | x_k] &\leq \mathbb{E}[\bar{e}_k | x_k] + 2V.
 \end{aligned} \tag{9}$$

To obtain our error bounds, we need the following preliminary results on the zeroth-order oracle.

Proposition 1 *Under Assumption 1(a),(c), the following holds.*

- (a) $\|\mathbb{E}[g_{\eta, k+}(x, u)] - \text{grad} f_{k+}(x)\| \leq \frac{L\eta}{2}(d+3)^{3/2} + \frac{\delta}{\eta}d^{1/2}$.
- (b) $\mathbb{E}[\|g_{\eta, k+}(x, u)\|^2] \leq \frac{L^2\eta^2}{2}(d+6)^3 + 2L\delta(d+4)^2 + \frac{2\delta^2}{\eta^2}d + 2(d+4)\|\text{grad} f_{k+}(x)\|^2$.

Proof See Appendix B. ■

Proposition 1 is the extension of (Li et al., 2020, Proposition 2.1) to the time-varying case. Note that our bounds depend on δ , which is the upper bound on the cost function variation by means of Assumption 1(c). We emphasise that Proposition 1 recovers the oracle bounds in (Li et al., 2020) for $\delta \rightarrow 0$ (time-invariant case).

We are now ready to present the main result, which is formalised in the theorem below.

Theorem 1 *Consider the iterates $x_{k+1} = \mathcal{P}_{\mathcal{X}}[\text{Exp}_{x_k}(-\alpha_k g_{\eta, k+}(x_k, u_k))]$ with $\alpha_k > 0$ and $g_{\eta, k+}$ as per (3). Then, under Assumption 1(a)–(d), we have that for all $k \geq 0$,*

$$\mathbb{E}[e_{k+1}|x_k] \leq \sqrt{\psi(e_k)} + 2V, \tag{10}$$

where

$$\begin{aligned}
 \psi(e_k) &:= (2(d+4)L^2\zeta(\kappa, e_k)\alpha_k^2 - \sigma\alpha_k + 1)e_k^2 \\
 &\quad + \alpha_k \left(L\eta(d+3)^{3/2} + \frac{2\delta}{\eta}d^{1/2} \right) e_k \\
 &\quad + \left(\frac{L^2\eta^2}{2}(d+6)^3 + 2L\delta(d+4)^2 + \frac{2\delta^2}{\eta^2}d \right) \zeta(\kappa, e_k)\alpha_k^2.
 \end{aligned}$$

Proof We take conditional expectations in (7) and obtain

$$\begin{aligned}
\mathbb{E} [\bar{e}_k^2 \mid x_k] &\leq e_k^2 + 2\alpha_k \langle \mathbb{E} [g_{\eta,k^+}(x_k, u_k) \mid x_k], \text{Exp}_{x_k}^{-1}(x_{k^+}^*) \rangle \\
&\quad + \zeta(\kappa, e_k) \alpha_k^2 \mathbb{E} \left[\|g_{\eta,k^+}(x_k, u_k)\|^2 \mid x_k \right] \\
&\leq e_k^2 + 2\alpha_k \langle \mathbb{E} [g_{\eta,k^+}(x_k, u_k)], \text{Exp}_{x_k}^{-1}(x_{k^+}^*) \rangle \\
&\quad + \zeta(\kappa, e_k) \alpha_k^2 \left(\frac{L^2 \eta^2}{2} (d+6)^3 + 2L\delta(d+4)^2 \right. \\
&\quad \left. + \frac{2\delta^2}{\eta^2} d + 2(d+4) \|\text{grad} f_{k^+}(x_k)\|^2 \right), \tag{11}
\end{aligned}$$

where the last inequality follows from Proposition 1(b). Note that

$$\begin{aligned}
&\langle \mathbb{E} [g_{\eta,k^+}(x_k, u_k)], \text{Exp}_{x_k}^{-1}(x_{k^+}^*) \rangle \\
&= \langle \mathbb{E} [g_{\eta,k^+}(x_k, u_k)] - \text{grad} f_{k^+}(x_k), \text{Exp}_{x_k}^{-1}(x_{k^+}^*) \rangle + \langle \text{grad} f_{k^+}(x_k), \text{Exp}_{x_k}^{-1}(x_{k^+}^*) \rangle.
\end{aligned}$$

Then, by the Cauchy-Scharwz inequality and (6),

$$\begin{aligned}
&\langle \mathbb{E} [g_{\eta,k^+}(x_k, u_k)], \text{Exp}_{x_k}^{-1}(x_{k^+}^*) \rangle \\
&\leq \|\mathbb{E} [g_{\eta,k^+}(x_k, u_k)] - \text{grad} f_{k^+}(x_k)\| \|\text{Exp}_{x_k}^{-1}(x_{k^+}^*)\| - \frac{\sigma}{2} \text{dist}(x_k, x_{k^+}^*)^2 \\
&= \|\mathbb{E} [g_{\eta,k^+}(x_k, u_k)] - \text{grad} f_{k^+}(x_k)\| e_k - \frac{\sigma}{2} e_k^2 \\
&\leq \left(\frac{L\eta}{2} (d+3)^{3/2} + \frac{\delta}{\eta} d^{1/2} \right) e_k - \frac{\sigma}{2} e_k^2, \tag{12}
\end{aligned}$$

where the last inequality follows from Proposition 1(a).

On the other hand, note that from (4) and the reverse triangle inequality,

$$\| \|\text{grad} f(x)\| - \|\Gamma_y^x \text{grad} f(y)\| \| \leq L \text{dist}(x, y),$$

which, in turn, implies that $\|\text{grad} f_{k^+}(x_k)\| \leq L e_k$. Therefore, by using the latter together with (12) into (11), we obtain

$$\begin{aligned}
\mathbb{E} [\bar{e}_k^2 \mid x_k] &\leq e_k^2 + 2\alpha_k \left(\left(\frac{L\eta}{2} (d+3)^{3/2} + \frac{\delta}{\eta} d^{1/2} \right) e_k - \frac{\sigma}{2} e_k^2 \right) \\
&\quad + \zeta(\kappa, e_k) \alpha_k^2 \left(\frac{L^2 \eta^2}{2} (d+6)^3 + 2L\delta(d+4)^2 + \frac{2\delta^2}{\eta^2} d + 2(d+4)L^2 e_k^2 \right) \\
&= (2(d+4)L^2 \zeta(\kappa, e_k) \alpha_k^2 - \sigma \alpha_k + 1) e_k^2 \\
&\quad + \alpha_k \left(L\eta(d+3)^{3/2} + \frac{2\delta}{\eta} d^{1/2} \right) e_k \\
&\quad + \left(\frac{L^2 \eta^2}{2} (d+6)^3 + 2L\delta(d+4)^2 + \frac{2\delta^2}{\eta^2} d \right) \zeta(\kappa, e_k) \alpha_k^2.
\end{aligned}$$

By Jensen's inequality we get $\mathbb{E} [\bar{e}_k \mid x_k]^2 \leq \mathbb{E} [\bar{e}_k^2 \mid x_k]$, and the proof is thus complete from applying (9). ■

The next corollary provides a choice of step size that ensures the expected tracking error remains bounded for $k \rightarrow \infty$.

Corollary 1 Under Assumption 1, if $\alpha_k = \alpha \in \left(0, \frac{\sigma}{2L^2(d+4)\zeta(\kappa, R)}\right)$ for all k , then

$$\limsup_{k \rightarrow \infty} \mathbb{E}[e_k] \leq \Delta := \frac{D + 2V}{1 - \rho},$$

where $\rho := \sqrt{2(d+4)L^2\zeta(\kappa, R)\alpha^2 - \sigma\alpha + 1}$, $D := \alpha \max\{\theta_1, \theta_2\}$, and

$$\theta_1 := \frac{L\eta(d+3)^{3/2} + (2/\eta)\delta d^{1/2}}{2\rho}, \quad \theta_2 := \sqrt{\left(\frac{L^2\eta^2}{2}(d+6)^3 + 2L\delta(d+4)^2 + \frac{2\delta^2}{\eta^2}d\right)\zeta(\kappa, R)}.$$

Proof See Appendix C. ■

Corollary 1 shows that we can closely follow the optimisers of the time-varying optimisation problem in (1) as k tends to infinity.

Remark 1 It is worth noticing that Δ in Corollary 1 depends on the manifold geometry through κ , which lower bounds the sectional curvature of \mathcal{M} . In fact, Δ is an increasing function of κ . Then, if we consider Δ as the measure of performance of the algorithm, we can conclude that negative manifold curvature has a detrimental effect on performance when compared to the Euclidean counterpart in which $\kappa = 0$. This is consistent with recent literature, for instance, in Riemannian SVRG algorithms, negative space curvature has an adverse effect on the convergence rate of the algorithm as observed in (Zhang et al., 2016), see also (Zhang and Sra, 2016) for similar conclusions on subgradient methods. It is worth pointing out that for $\kappa = 0$ (i.e. $\mathcal{M} \equiv \mathbb{R}^n$), Δ reduces to the bound presented in (Shames et al., 2019). In addition, we emphasise that Δ depends on the intrinsic dimension d of the manifold, and not on the ambient space dimension n .

To finish up this section, we provide choices for the parameters η and α , that is, oracle's precision and step size, so that the performance metric Δ is minimised.

Theorem 2 Let $\bar{\eta} := (4\delta^2 d / (L^2(d+6)^3))^{1/4}$, and $\bar{\alpha}$ be the root² of $A\alpha^2 + B\alpha + C = 0$ in the interval $\left(0, \frac{\sigma}{2L^2(d+4)\zeta(\kappa, R)}\right)$ with

$$\begin{aligned} A &:= (8VL^2\zeta(\kappa, R)(d+4) + \sigma\bar{\theta})^2 - 8\bar{\theta}^2L^2\zeta(\kappa, R)(d+4), \\ B &:= -4V(\bar{\theta}\sigma^2 + 8VL^2\zeta(\kappa, R)(d+4)\sigma + 8\bar{\theta}L^2\zeta(\kappa, R)(d+4)), \\ C &:= (2\sigma V + 2\bar{\theta})^2 - 4\bar{\theta}^2, \\ \bar{\theta} &:= \sqrt{\left(\frac{L^2\bar{\eta}^2}{2}(d+6)^3 + 2L\delta(d+4)^2 + \frac{2\delta^2}{\bar{\eta}^2}d\right)\zeta(\kappa, R)}. \end{aligned}$$

Then, $\bar{\eta}$ and $\bar{\alpha}$ minimise Δ in Corollary 1.

Proof See Appendix D. ■

²We note that the choice of step size $\bar{\alpha}$ in Theorem 2 always exists since $\Delta|_{\eta=\bar{\eta}}$ is convex in α over the interval $\left(0, \frac{\sigma}{2L^2(d+4)\zeta(\kappa, R)}\right)$.

3.2 A discussion on regret bounds

In this section, we provide some remarks on regret bounds for our setting, for which we impose an extra assumption on the gradient.

Assumption 2 For all $f \in \mathcal{F}$ and $x \in \mathcal{X}$, $\exists G > 0$ such that $\|\text{grad}f(x)\| \leq G$.

Consider the following regrets, as a counterpart to our tracking and estimation errors respectively,

$$\begin{aligned} \text{Reg}_T^{\text{Track.}} &:= \sum_{k=0}^T \mathbb{E} [f_{k+}(x_k)] - f_{k+}(x_{k+}^*), \\ \text{Reg}_T^{\text{Est.}} &:= \sum_{k=0}^T \mathbb{E} [f_{k+}(x_{k+1})] - f_{k+}(x_{k+}^*). \end{aligned}$$

The geodesic strong convexity of f_{k+} , the Cauchy-Schwarz inequality, and Assumption 1 imply

$$\begin{aligned} f_{k+}(x_k) - f_{k+}(x_{k+}^*) &\leq -\langle \text{grad}f_{k+}(x_k), \text{Exp}_{x_k}^{-1}(x_{k+}^*) \rangle \\ &\leq \|\text{grad}f_{k+}(x_k)\| e_k \\ &\leq G e_k \\ \mathbb{E} [f_{k+}(x_k)] - f_{k+}(x_{k+}^*) &\leq G \mathbb{E} [e_k]. \end{aligned}$$

Similarly, it is immediate to show that $\mathbb{E} [f_{k+}(x_{k+1})] - f_{k+}(x_{k+}^*) \leq G \mathbb{E} [\bar{e}_k]$. Consider the step size is chosen as $\alpha_k = \alpha \in \left(0, \frac{\sigma}{2L^2(d+4)\zeta(\kappa, R)}\right)$ for all k , like in Corollary 1. We can now obtain upper bounds on $\text{Reg}_T^{\text{Track.}}$ and $\text{Reg}_T^{\text{Est.}}$ by means of Lemmas 6 and 7 in Appendix E. That is,

$$\begin{aligned} \text{Reg}_T^{\text{Track.}} &\leq \frac{G}{1-\rho} (\mathbb{E} [e_0] - \rho \mathbb{E} [e_T] + TD + V_T), \\ \text{Reg}_T^{\text{Est.}} &\leq \frac{G}{1-\rho} (\mathbb{E} [\bar{e}_0] - \rho \mathbb{E} [\bar{e}_T] + TD + \rho V_T), \end{aligned}$$

where $V_T := \sum_{k=0}^{T-1} \text{dist}(x_{k+}^*, x_{k+1}^*)$, and ρ, D are as per Corollary 1. Next, we note that if we choose the oracle's precision η such that $D \leq \bar{c}/\sqrt{T}$ for some positive constant \bar{c} , then

$$\text{Reg}_T^{\text{Track.}} \leq \frac{G}{1-\rho} \left(\mathbb{E} [e_0] - \rho \mathbb{E} [e_T] + \bar{c}\sqrt{T} + V_T \right), \quad (13a)$$

$$\text{Reg}_T^{\text{Est.}} \leq \frac{G}{1-\rho} \left(\mathbb{E} [\bar{e}_0] - \rho \mathbb{E} [\bar{e}_T] + \bar{c}\sqrt{T} + \rho V_T \right), \quad (13b)$$

which are sub-linear in T provided V_T is also sub-linear. Of course this choice of η relies on the knowledge of T , and an interesting future direction is to study the interplay between the step size α and the oracle's precision η so that the regret is sub-linear in T without requiring α and η to depend on T .

4 Experiments

To validate our results, we apply our zeroth-order algorithm to the problem of computing the Karcher mean of a collection of symmetric positive definite (SPD) matrices, also known as Riemannian centre of mass or Fréchet mean (Bini and Iannazzo, 2013). This problem appears in a

number of applications such as medical imaging (Fletcher and Joshi, 2007), image segmentation (Rathi et al., 2007), signal estimation (Kurtek et al., 2011), and particle filtering (Bordin Jr et al., 2018). Note that the Karcher mean is guaranteed to exist and be unique on a Hadamard manifold (Berger, 2012).

We consider a time-varying version of the Karcher mean problem which arises in online scenarios. For instance, we may want to find a central representative for a collection of online noisy measurements of a moving object. Formally, we consider that the measurements are N SPD matrices of dimension $m \times m$ that become available at each time k , which we denote by $\{A_{k,1}, \dots, A_{k,N}\}$.

The manifold of SPD matrices is defined as $\mathcal{M} := \{X \in \mathbb{R}^{m \times m} : X = X^\top \succ 0\}$. If we equip \mathcal{M} with the Riemannian metric

$$\langle M, N \rangle_X := \text{Tr} \{X^{-1} M X^{-1} N\}, \quad M, N \in T_X \mathcal{M},$$

for every $X \in \mathcal{M}$, then the SPD manifold is a Hadamard manifold (Bacák, 2014). The Riemannian distance is given by

$$\text{dist}(X, Y) := \left\| \log \left(X^{-1/2} Y X^{-1/2} \right) \right\|_F,$$

where $\|\cdot\|_F$ corresponds to the Euclidean (or Frobenius) norm, and the exponential mapping is

$$\text{Exp}_X(M) = X^{1/2} \exp \left(X^{-1/2} M X^{-1/2} \right) X^{1/2}, \quad M \in T_X \mathcal{M},$$

for every $X \in \mathcal{M}$, where \exp denotes the matrix exponential. The time-varying cost function is defined as

$$f_k(X) := \frac{1}{2N} \sum_{i=1}^N \text{dist}(X, A_{k,i})^2, \quad k \in \mathbb{N}_0. \quad (14)$$

The Karcher mean for each set of measurements $\{A_{k,i}\}_{i=1}^N$ received at time k is the unique minimiser of $f_k(X)$, i.e. $x_k^* := \arg \min_{X \in \mathcal{M}} f_k(X)$, for all $k \in \mathbb{N}_0$. The cost function (14) is known to be geodesically strongly convex with $\sigma = 1$ and geodesically ζ -smooth, see e.g. (Zhang and Sra, 2016; Zhang et al., 2016). We note that (14) corresponds to the case where $f_{k+} = f_k$ in Assumption 1(c), i.e. $\delta \rightarrow 0$, and we use $\delta = 0.001$. We consider $N = 10$, two problem sizes $m \in \{3, 9\}$, and the manifold dimension is $d = m(m+1)/2$. For this example, we estimated $V = 0.5$ and $\zeta = 1.5$. The step size and oracle's precision for each $m \in \{3, 9\}$ are chosen as per Theorem 2, which gives $\bar{\alpha}_3 = 0.0074$, $\bar{\alpha}_9 = 0.0015$, and $\bar{\eta}_3 = 0.0089$ and $\bar{\eta}_9 = 0.005$. The matrices $\{A_{k,i}\}_{i=1}^N$ were randomly generated using the MANOPT toolbox in MATLAB, see (Boumal et al., 2014).

Figure 2 depicts the average tracking error $\mathbb{E}[e_k]$ after implementing our zeroth-order algorithm for 100 random runs and different values of problem size. We can see that the average tracking errors converge to a ball which is upper bounded by Δ for $k \rightarrow \infty$. The theoretical asymptotic bounds from Corollary 1 are $\Delta_3 = 543.73$ and $\Delta_9 = 2666$ for $m = 3$ and $m = 9$, respectively. Comparing with the values in Figure 2, we can conclude that these bounds can become conservative. Obtaining less conservative bounds is an open question for future research. We note that one source of conservatism in comparison to the Euclidean case is the law of cosines in Lemma 5.

5 Conclusions

A gradient-free algorithm for the minimisation of time-varying cost functions on Hadamard manifolds was proposed. Bounds on the expectation of the tracking error were derived, and choices

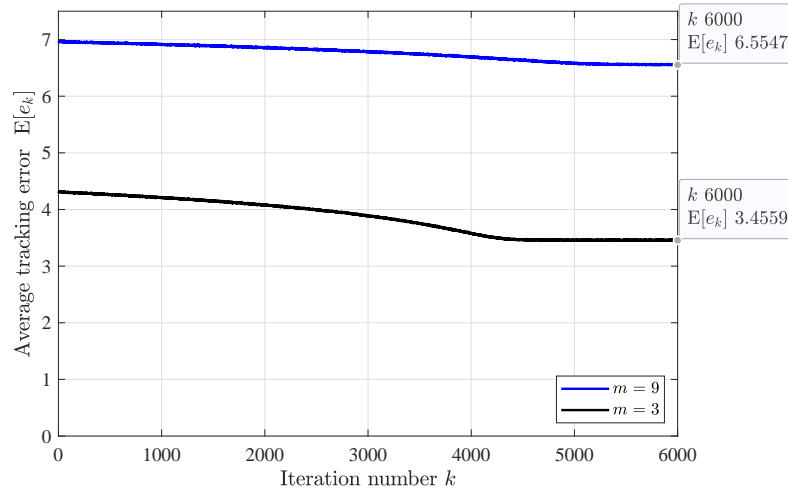


Figure 2: Algorithm’s average tracking error—over 100 random scenarios—for different values of problem size.

for algorithm parameters such that the asymptotic tracking error bound is minimised were provided. Remarks on regret bounds were also given. Finally, the theoretical results were validated via numerical experiments.

Future work includes the extension to a more general class of Riemannian manifolds by trying to relax the way we sample the random vector u in (3), and also the extension to the non-smooth time-varying case. In addition, looking at the problem in a different set of coordinates at each step is also an interesting future direction. Lastly, exploring different gradient approximations in the oracle for this time-varying context is also of interest.

References

- P.-A. Absil, R. Mahony, and R. Sepulchre. *Optimization algorithms on matrix manifolds*. Princeton University Press, 2009.
- M. Bacák. *Convex analysis and optimization in Hadamard spaces*, volume 22. Walter de Gruyter GmbH & Co KG, 2014.
- M. Berger. *A panoramic view of Riemannian geometry*. Springer Science & Business Media, 2012.
- O. Besbes, Y. Gur, and A. Zeevi. Non-stationary stochastic optimization. *Operations research*, 63(5):1227–1244, 2015.
- D. A. Bini and B. Iannazzo. Computing the karcher mean of symmetric positive definite matrices. *Linear Algebra and its Applications*, 438(4):1700–1710, 2013.
- R. L. Bishop and B. O’Neill. Manifolds of negative curvature. *Transactions of the American Mathematical Society*, 145:1–49, 1969.
- S. Bonnabel. Stochastic gradient descent on Riemannian manifolds. *IEEE Transactions on Automatic Control*, 58(9):2217–2229, 2013.

- C. J. Bordin Jr, C. G. de Figueredo, and M. G. Bruno. Nonlinear state estimation on unit spheres using manifold particle filtering. *Digital Signal Processing*, 81:50–56, 2018.
- N. Boumal, B. Mishra, P.-A. Absil, and R. Sepulchre. Manopt, a matlab toolbox for optimization on manifolds. *The Journal of Machine Learning Research*, 15(1):1455–1459, 2014.
- N. Boumal, P.-A. Absil, and C. Cartis. Global rates of convergence for nonconvex optimization on manifolds. *IMA Journal of Numerical Analysis*, 39(1):1–33, 2019.
- S. Bubeck and N. Cesa-Bianchi. Regret analysis of stochastic and nonstochastic multi-armed bandit problems. *arXiv preprint arXiv:1204.5721*, 2012.
- A. Chattopadhyay, S. E. Selvan, and U. Amato. A derivative-free Riemannian Powell’s method, minimizing hartley-entropy-based ICA contrast. *IEEE transactions on neural networks and learning systems*, 27(9):1983–1990, 2015.
- P.-Y. Chen, H. Zhang, Y. Sharma, J. Yi, and C.-J. Hsieh. Zoo: Zeroth order optimization based black-box attacks to deep neural networks without training substitute models. In *Proceedings of the 10th ACM Workshop on Artificial Intelligence and Security*, pages 15–26, 2017.
- S. Chen, Z. Deng, S. Ma, and A. M.-C. So. Manifold proximal point algorithms for dual principal component pursuit and orthogonal dictionary learning. In *2019 53rd Asilomar Conference on Signals, Systems, and Computers*, pages 259–263. IEEE, 2019.
- S. Chen, S. Ma, A. Man-Cho So, and T. Zhang. Proximal gradient method for nonsmooth optimization over the Stiefel manifold. *SIAM Journal on Optimization*, 30(1):210–239, 2020.
- T. Chen and G. B. Giannakis. Bandit convex optimization for scalable and dynamic IoT management. *IEEE Internet of Things Journal*, 6(1):1276–1286, 2018.
- C.-K. Chiang, C.-J. Lee, and C.-J. Lu. Beating bandits in gradually evolving worlds. In *Conference on Learning Theory*, pages 210–227, 2013.
- R. Dixit, A. S. Bedi, R. Tripathi, and K. Rajawat. Online learning with inexact proximal online gradient descent algorithms. *IEEE Transactions on Signal Processing*, 67(5):1338–1352, 2019.
- P. T. Fletcher and S. Joshi. Riemannian geometry for the statistical analysis of diffusion tensor data. *Signal Processing*, 87(2):250–262, 2007.
- R. S. Fong and P. Tino. Stochastic derivative-free optimization on Riemannian manifolds. *arXiv preprint arXiv:1908.06783*, 2019.
- E. Hazan. Introduction to online convex optimization. *arXiv preprint arXiv:1909.05207*, 2019.
- A. S. Ira, C. Manzie, I. Shames, R. Chin, D. Nešić, H. Nakada, and T. Sano. Tuning of multivariable model predictive controllers through expert bandit feedback. *International Journal of Control*, pages 1–9, 2020.
- H. Kasai, H. Sato, and B. Mishra. Riemannian stochastic recursive gradient algorithm. In *International Conference on Machine Learning*, pages 2516–2524, 2018.
- A. Kovnatsky, K. Glashoff, and M. M. Bronstein. MADMM: a generic algorithm for non-smooth optimization on manifolds. In *European Conference on Computer Vision*, pages 680–696. Springer, 2016.

- S. A. Kurtsek, A. Srivastava, and W. Wu. Signal estimation under random time-warpings and nonlinear signal alignment. In *Advances in Neural Information Processing Systems*, pages 675–683, 2011.
- J. Li, K. Balasubramanian, and S. Ma. Zeroth-order optimization on Riemannian manifolds. *arXiv preprint arXiv:2003.11238*, 2020.
- X. Li, S. Chen, Z. Deng, Q. Qu, Z. Zhu, and A. M. C. So. Weakly convex optimization over Stiefel manifold using Riemannian subgradient-type methods. *arXiv*, pages arXiv–1911, 2019.
- D. Malik, A. Pananjady, K. Bhatia, K. Khamaru, P. Bartlett, and M. Wainwright. Derivative-free methods for policy optimization: Guarantees for linear quadratic systems. In *The 22nd International Conference on Artificial Intelligence and Statistics*, pages 2916–2925. PMLR, 2019.
- H. Mania, A. Guy, and B. Recht. Simple random search of static linear policies is competitive for reinforcement learning. In *Advances in Neural Information Processing Systems*, pages 1800–1809, 2018.
- J. H. Manton. Optimization algorithms exploiting unitary constraints. *IEEE Transactions on Signal Processing*, 50(3):635–650, 2002.
- Y. Nesterov and V. Spokoiny. Random gradient-free minimization of convex functions. *Foundations of Computational Mathematics*, 17(2):527–566, 2017.
- M. J. Powell. An efficient method for finding the minimum of a function of several variables without calculating derivatives. *The computer journal*, 7(2):155–162, 1964.
- Y. Rathi, A. Tannenbaum, and O. Michailovich. Segmenting images on the tensor manifold. In *2007 IEEE Conference on Computer Vision and Pattern Recognition*, pages 1–8. IEEE, 2007.
- I. Shames, D. Selvaratnam, and J. H. Manton. Online optimization using zeroth order oracles. *IEEE Control Systems Letters*, 4(1):31–36, 2019.
- A. Simonetto, E. Dall’Anese, S. Paternain, G. Leus, and G. B. Giannakis. Time-varying convex optimization: Time-structured algorithms and applications. *Proceedings of the IEEE*, 2020.
- J. Sun, Q. Qu, and J. Wright. Complete dictionary recovery over the sphere ii: Recovery by Riemannian trust-region method. *IEEE Transactions on Information Theory*, 63(2):885–914, 2016.
- B. Vandereycken. Low-rank matrix completion by Riemannian optimization. *SIAM Journal on Optimization*, 23(2):1214–1236, 2013.
- B. Wang, S. Ma, and L. Xue. Riemannian stochastic proximal gradient methods for nonsmooth optimization over the Stiefel manifold. *arXiv preprint arXiv:2005.01209*, 2020.
- M. Weber and S. Sra. Projection-free nonconvex stochastic optimization on Riemannian manifolds. *arXiv preprint arXiv:1910.04194*, 2019.
- T. Yang, L. Zhang, R. Jin, and J. Yi. Tracking slowly moving clairvoyant: Optimal dynamic regret of online learning with true and noisy gradient. In *International Conference on Machine Learning*, pages 449–457, 2016.

H. Zhang and S. Sra. First-order methods for geodesically convex optimization. In *Conference on Learning Theory*, pages 1617–1638, 2016.

H. Zhang, S. J. Reddi, and S. Sra. Riemannian SVRG: Fast stochastic optimization on Riemannian manifolds. In *Advances in Neural Information Processing Systems*, pages 4592–4600, 2016.

P. Zhou, X. Yuan, S. Yan, and J. Feng. Faster first-order methods for stochastic non-convex optimization on Riemannian manifolds. *IEEE transactions on pattern analysis and machine intelligence*, 2019.

A Technical lemmas

Lemma 2 (Bacák (2014)) *Let \mathcal{M} be a Hadamard manifold and $\mathcal{X} \subset \mathcal{M}$ a closed convex set. Then, the mapping $\mathcal{P}_{\mathcal{X}}(x) := \{y \in \mathcal{X} : \text{dist}(x, z) = \inf_{z \in \mathcal{X}} \text{dist}(x, z)\}$ is single-valued and nonexpansive, that is, we have $\text{dist}(\mathcal{P}_{\mathcal{X}}(x), \mathcal{P}_{\mathcal{X}}(y)) \leq \text{dist}(x, y)$ for every $x, y \in \mathcal{M}$.*

Lemma 3 (Shames et al. (2019)) *Let $x, y, a, c \geq 0$ and $b \in \mathbb{R}$. Then $x^2 \leq ay^2 + by + c$ implies $x \leq y\sqrt{a} + D$, where $D := \max\left\{\frac{b}{2\sqrt{a}}, \sqrt{c}\right\}$.*

Lemma 4 (Li et al. (2020)) *Suppose \mathcal{X} is a d -dimensional subspace of \mathbb{R}^n , with orthogonal projection matrix $P \in \mathbb{R}^{n \times n}$, $u_0 \sim \mathcal{N}(0, I_n)$, and $u = Pu_0$ is the orthogonal projection of u_0 onto \mathcal{X} . Then,*

(a) $x = \frac{1}{\nu} \int_{\mathbb{R}^n} \langle x, u \rangle u e^{-\frac{1}{2}\|u_0\|^2} du_0, \forall x \in \mathcal{X}.$

(b) For $p \in [0, 2]$, $\mathbb{E}[\|u\|^p] \leq d^{p/2}$, and if $p \geq 2$, then $\mathbb{E}[\|u\|^p] \leq (d + p)^{p/2}$.

(c) $\mathbb{E}\left[\|\langle \text{grad} f_{k^+}(x), u \rangle u\|^2\right] \leq (d + 4) \|\text{grad} f_{k^+}(x)\|^2.$

Lemma 5 (Zhang and Sra (2016)) *If a, b, c are the sides (i.e. lengths) of a geodesic triangle in an Alexandrov space with curvature lower bounded by κ , and A is the angle between sides b and c , then*

$$a^2 \leq \frac{c\sqrt{|\kappa|}}{\tanh(c\sqrt{|\kappa|})} b^2 + c^2 - 2bc \cos(A).$$

B Proof of Proposition 1

(a) We complete the proof with the following steps.

$$\begin{aligned}
& \left\| \mathbb{E} [g_{\eta, k^+}(x, u)] - \text{grad} f_{k^+}(x) \right\| \\
& \stackrel{\text{Lemma 4(a)}}{=} \left\| \frac{1}{\nu} \int_{\mathbb{R}^n} \left(\frac{f_{k^+}(\text{Exp}_x(\eta u)) - f_k(x)}{\eta} - \langle \text{grad} f_{k^+}(x), u \rangle \right) u e^{-\frac{1}{2}\|u_0\|^2} du_0 \right\| \\
& \leq \frac{1}{\eta\nu} \int_{\mathbb{R}^n} |f_{k^+}(\text{Exp}_x(\eta u)) - f_{k^+}(x) - \langle \text{grad} f_{k^+}(x), \eta u \rangle \\
& \quad + f_{k^+}(x) - f_k(x)| \|u\| e^{-\frac{1}{2}\|u_0\|^2} du_0 \\
& \stackrel{\text{Assum. 1(a),(c)}}{\leq} \frac{1}{\eta\nu} \int_{\mathbb{R}^n} \left(\frac{L\eta^2}{2} \|u\|^2 + \delta \right) \|u\| e^{-\frac{1}{2}\|u_0\|^2} du_0 \\
& = \frac{L\eta}{2\nu} \int_{\mathbb{R}^n} \|u\|^3 e^{-\frac{1}{2}\|u_0\|^2} du_0 + \frac{\delta}{\eta\nu} \int_{\mathbb{R}^n} \|u\| e^{-\frac{1}{2}\|u_0\|^2} du_0 \\
& \stackrel{\text{Lemma 4(b)}}{\leq} \frac{L\eta}{2} (d+3)^{3/2} + \frac{\delta}{\eta} d^{1/2}.
\end{aligned}$$

(b) From Assumptions 1(a) and 1(c)

$$\begin{aligned}
(f_{k^+}(\text{Exp}_x(\eta u)) - f_k(x))^2 &= (f_{k^+}(\text{Exp}_x(\eta u)) - f_{k^+}(x) - \langle \text{grad} f_{k^+}(x), \eta u \rangle \\
& \quad + f_{k^+}(x) - f_k(x) + \langle \text{grad} f_{k^+}(x), \eta u \rangle)^2 \\
& \leq \left(\frac{L\eta^2}{2} \|u\|^2 + \delta + \langle \text{grad} f_{k^+}(x), \eta u \rangle \right)^2 \\
& \leq 2 \left(\frac{L\eta^2}{2} \|u\|^2 + \delta \right)^2 + 2\eta \langle \text{grad} f_{k^+}(x), u \rangle^2.
\end{aligned}$$

Consequently,

$$\begin{aligned}
\mathbb{E} \left[\|g_{\eta, k^+}(x, u)\|^2 \right] &= \frac{(f_{k^+}(\text{Exp}_x(\eta u)) - f_k(x))^2}{\eta^2} \mathbb{E} \left[\|u\|^2 \right] \\
&\leq \frac{L^2\eta^2}{2} \mathbb{E} \left[\|u\|^6 \right] + 2L\delta \mathbb{E} \left[\|u\|^4 \right] + \frac{2\delta^2}{\eta^2} \mathbb{E} \left[\|u\|^2 \right] \\
&\quad + 2\mathbb{E} \left[\|\langle \text{grad} f_{k^+}(x), u \rangle u\|^2 \right].
\end{aligned}$$

The proof is thus complete by means of Lemma 4(b),(c).

C Proof of Corollary 1

First note that Assumption 1(e) implies that $\zeta(\kappa, e_k) \leq \zeta(\kappa, R)$. Then, for $\alpha_k = \alpha$,

$$\begin{aligned} \psi(e_k) = & \underbrace{(2(d+4)L^2\zeta(\kappa, R)\alpha^2 - \sigma\alpha + 1)}_{:=a} e_k^2 \\ & + \alpha \underbrace{\left(L\eta(d+3)^{3/2} + \frac{2\delta}{\eta}d^{1/2} \right)}_{:=b} e_k \\ & + \underbrace{\left(\frac{L^2\eta^2}{2}(d+6)^3 + 2L\delta(d+4)^2 + \frac{2\delta^2}{\eta^2}d \right)}_{:=c} \zeta(\kappa, R)\alpha^2. \end{aligned}$$

Next, from the proof of Theorem 1 we know that $\mathbb{E}[\bar{e}_k | x_k]^2 \leq \psi(e_k) = ae_k^2 + be_k + c$. Therefore, Lemma 3 implies $\mathbb{E}[\bar{e}_k | x_k] \leq \rho e_k + D$. We then use the latter inequality in (9) to get $\mathbb{E}[e_{k+1} | x_k] \leq \rho e_k + D + 2V$. Applying expectation to this leads to

$$\mathbb{E}[e_{k+1}] \leq \rho \mathbb{E}[e_k] + D + 2V, \quad (15)$$

Then, for $0 < \alpha < \frac{\sigma}{2L^2(d+4)\zeta(\kappa, R)}$, we have that $\rho < 1$ and thus the result follows immediately from (15).

D Proof of Theorem 2

Note that $\rho^2 = 2(d+4)L^2\zeta(\kappa, R)\alpha^2 - \sigma\alpha + 1 > \frac{L^2}{2}\alpha^2 - \sigma\alpha + 1 \geq \frac{\sigma^2}{2}\alpha^2 - \sigma\alpha + 1$, where the last inequality follows from Assumption 1(a). Then, $2\rho^2 > (\sigma\alpha)^2 - 2\sigma\alpha + 2 = (\sigma\alpha - 1)^2 + 1 \geq 1$, which implies that $2\rho > \sqrt{2}$. Therefore,

$$\theta_1 = \frac{L\eta(d+3)^{3/2} + (2/\eta)\delta d^{1/2}}{2\rho} < \frac{L\eta(d+3)^{3/2} + (2/\eta)\delta d^{1/2}}{\sqrt{2}},$$

and thus

$$\theta_1^2 < \frac{L^2\eta^2}{2}(d+3)^3 + 2L\delta d^{1/2}(d+3)^{3/2} + \frac{2\delta^2}{\eta^2}d. \quad (16)$$

On the other hand,

$$\theta_2^2 = \frac{L^2\eta^2}{2}\zeta(\kappa, R)(d+6)^3 + 2L\delta\zeta(\kappa, R)(d+4)^2 + \frac{2\delta^2}{\eta^2}\zeta(\kappa, R)d,$$

and note that, by definition, $\zeta(\kappa, R) \geq 1$ for all κ and R . We also note that $(d+4)^2 > d^{1/2}(d+3)^{3/2}$ for all $d \geq 0$. Hence,

$$\begin{aligned} \theta_2^2 & \geq \frac{L^2\eta^2}{2}(d+6)^3 + 2L\delta(d+4)^2 + \frac{2\delta^2}{\eta^2}d \\ & > \frac{L^2\eta^2}{2}(d+3)^3 + 2L\delta d^{1/2}(d+3)^{3/2} + \frac{2\delta^2}{\eta^2}d \\ & \stackrel{(16)}{>} \theta_1^2, \end{aligned}$$

which implies that $D = \alpha \max\{\theta_1, \theta_2\} = \alpha\theta_2$, and thus $\Delta = \frac{\alpha\theta_2 + 2V}{1-\rho}$. We note that Δ depends on η through θ_2 only, and it depends on α through ρ only. We can see that

$$\frac{\partial\theta_2}{\partial\eta} = 0 \implies \zeta(\kappa, R) \left(L^2(d+6)^3\bar{\eta} - \frac{4\delta^2 d}{\bar{\eta}^3} \right) = 0,$$

from which we conclude that $\bar{\eta} = (4\delta^2 d / (L^2(d+6)^3))^{1/4}$ minimises θ_2 , and since the denominator of Δ is independent of η , Δ attains its minimum at $\bar{\eta}$.

Next, we obtain $\bar{\alpha}$ that minimises Δ . To that end, we compute the derivative of Δ evaluated at $\bar{\eta}$ with respect to α and set it to be equal to zero. Note that

$$\frac{\partial\Delta|_{\eta=\bar{\eta}}}{\partial\alpha} = \frac{\partial}{\partial\alpha} \left(\frac{\alpha\bar{\theta} + 2V}{1 - \sqrt{2(d+4)L^2\zeta(\kappa, R)\alpha^2 - \sigma\alpha + 1}} \right) = 0$$

implies

$$2\bar{\theta}\sqrt{2L^2(d+4)\zeta(\kappa, R)\alpha^2 - \sigma\alpha + 1} + 8L^2V\zeta(\kappa, R)(d+4)\alpha + \sigma\bar{\theta}\alpha - 2\sigma V - 2\bar{\theta} = 0,$$

and then

$$((8L^2V\zeta(\kappa, R)(d+4) + \sigma\bar{\theta})\alpha - (2\sigma V + 2\bar{\theta}))^2 = 4\bar{\theta}^2 (2L^2(d+4)\zeta(\kappa, R)\alpha^2 - \sigma\alpha + 1). \quad (17)$$

Lastly, we simply group terms in (17) to write $A\alpha^2 + B\alpha + C = 0$ with A, B and C as per the theorem statement, completing the proof.

E Lemmas for Section 3.2

Lemma 6 *Let $\alpha_k = \alpha \in \left(0, \frac{\sigma}{2L^2(d+4)\zeta(\kappa, R)}\right)$ for all k , then*

$$\sum_{k=0}^T \mathbb{E}[e_k] \leq \frac{1}{1-\rho} (\mathbb{E}[e_0] - \rho\mathbb{E}[e_T] + TD + V_T),$$

where $V_T := \sum_{k=0}^{T-1} \text{dist}(x_{k+}^*, x_{k+1}^*)$.

Proof We know that $e_{k+1} \leq \bar{e}_k + \text{dist}(x_{k+}^*, x_{k+1}^*)$, and thus $\mathbb{E}[e_{k+1} | x_k] \leq \mathbb{E}[\bar{e}_k | x_k] + \text{dist}(x_{k+}^*, x_{k+1}^*)$. Note that this is a relaxed version of (9) since we do not use the change on minimiser bound from Assumption 1(b). Therefore, from the proof of Corollary 1 we get that for $\alpha_k = \alpha \in \left(0, \frac{\sigma}{2L^2(d+4)\zeta(\kappa, R)}\right)$,

$$\mathbb{E}[e_{k+1}] \leq \rho\mathbb{E}[e_k] + D + \text{dist}(x_{k+}^*, x_{k+1}^*). \quad (18)$$

Summing both sides of (18) over and adding $\mathbb{E}[e_0]$ to both sides,

$$\begin{aligned} \sum_{k=0}^T \mathbb{E}[e_k] &\leq \mathbb{E}[e_0] + \rho \sum_{k=1}^T \mathbb{E}[e_{k-1}] + \sum_{k=1}^T D + \sum_{k=1}^T \text{dist}(x_{k-1}^*, x_k^*) \\ &= \mathbb{E}[e_0] + \rho \sum_{k=0}^{T-1} \mathbb{E}[e_k] + TD + \sum_{k=0}^{T-1} \text{dist}(x_{k+}^*, x_{k+1}^*) \\ &= \mathbb{E}[e_0] - \rho\mathbb{E}[e_T] + \rho \sum_{k=0}^T \mathbb{E}[e_k] + TD + \sum_{k=0}^{T-1} \text{dist}(x_{k+}^*, x_{k+1}^*) \\ &\leq \frac{1}{1-\rho} \left(\mathbb{E}[e_0] - \rho\mathbb{E}[e_T] + TD + \sum_{k=0}^{T-1} \text{dist}(x_{k+}^*, x_{k+1}^*) \right) \end{aligned}$$

■

Lemma 7 Let $\alpha_k = \alpha \in \left(0, \frac{\sigma}{2L^2(d+4)\zeta(\kappa, R)}\right)$ for all k , then

$$\sum_{k=0}^T \mathbb{E}[\bar{e}_k] \leq \frac{1}{1-\rho} (\mathbb{E}[\bar{e}_0] - \rho \mathbb{E}[\bar{e}_T] + TD + \rho V_T),$$

where $E_T := \sum_{k=0}^{T-1} D_k$, and $V_T := \sum_{k=0}^{T-1} \text{dist}(x_{k+}^*, x_{k+1}^*)$.

Proof From the proof of Corollary 1, we know that $\mathbb{E}[\bar{e}_k] \leq \rho \mathbb{E}[e_k] + D$. Then, by the triangle inequality of the Riemannian distance, we can write $e_k = \text{dist}(x_k, x_{k+}^*) \leq \text{dist}(x_k, x_{k+1}^*) + \text{dist}(x_{k+1}^*, x_{k+}^*)$. Therefore,

$$\mathbb{E}[\bar{e}_k] \leq \rho \mathbb{E}[\bar{e}_{k-1}] + \rho \text{dist}(x_{k+1}^*, x_{k+}^*) + D.$$

We proceed similarly to the proof of Lemma 6, that is,

$$\begin{aligned} \sum_{k=0}^T \mathbb{E}[\bar{e}_k] &\leq \mathbb{E}[\bar{e}_0] + \rho \sum_{k=0}^{T-1} \mathbb{E}[\bar{e}_k] + \rho \sum_{k=1}^T \text{dist}(x_{k+1}^*, x_{k+}^*) + TD \\ &= \mathbb{E}[\bar{e}_0] - \rho \mathbb{E}[\bar{e}_T] + \rho \sum_{k=0}^T \mathbb{E}[\bar{e}_k] + \rho \sum_{k=0}^{T-1} \text{dist}(x_{k+}^*, x_{k+1}^*) + TD \\ &\leq \frac{1}{1-\rho} (\mathbb{E}[\bar{e}_0] - \rho \mathbb{E}[\bar{e}_T] + TD + \rho V_T) \end{aligned}$$

■